Hindawi
Mathematical Problems in Engineering
Volume 2019, Article ID 9641723, 11 pages
https://doi.org/10.1155/2019/9641723

Research Article

Analysis and Tuning for Active Disturbance Rejection Control

Fan Wang,[1,2] Ran-Jun Wang ,[1,2] and En-Hai Liu[1,2]

[1]*Institute of Optics and Electronics of Chinese Academy of Sciences, Chengdu, China*
[2]*University of Chinese Academy of Sciences, Beijing, China*

Correspondence should be addressed to Ran-Jun Wang; wrjwzf@163.com

Received 13 March 2019; Revised 27 June 2019; Accepted 17 July 2019; Published 20 August 2019

Academic Editor: Martin Velasco Villa

The linear active disturbance rejection control (LADRC) method is investigated in this paper. Firstly, the integral effect of the ADRC is analyzed under the premise that ADRC was transformed into a new form. Then, ADRC is changed into an internal model control (IMC) framework, and an almost necessary and sufficient condition for stability and tracking performance of the ADRC system are proposed on this basis. In addition, some useful corollaries are proposed so that the traditional open-loop frequency-domain analysis method can be applied to ADRC system stability analysis. It also provides a theoretical principle and theoretical guidance for some parameter tuning. To improve the performance of ADRC, an approximate integral gain is treated as a separated adjustable parameter according to the new structure. Furthermore, tuning of some parameters is discussed to enhance system performance. Finally, simulations are used to verify the effectiveness of proposed methods.

1. Introduction

Model uncertainties and external disturbances are widely found in the industrial control system, which makes the modern control theory based on accurate models difficult to apply so that the classical PID control method still dominates the entire industrial control field. However, the classical PID control has some drawbacks, such as overshoot and limited antidisturbance capability. Therefore, PID control may not achieve the expected performance of complex systems. Active disturbance rejection control (ADRC) is a control technique proposed by Prof. Han [1, 2]. The main idea is that the model uncertainty and external disturbance are reduced to total disturbance, and the extended state observer (ESO) is used to estimate this total disturbance. Then, the state error feedback (SEF) is used to compensate the disturbance to achieve the dynamic linearization of the control system and implement the feedback control. As a practical alternative approach, the ADRC strategy has prominent performance in the control of linear and nonlinear uncertain systems, such as uncertain nonaffine-in-control nonlinear systems [3], induction motor systems [4], parallel active power filters [5], load frequency control [6], circular curved beam [7], two-mass drive systems [8], permanent magnet synchronous motors [9], diesel engines [10], buck-boost-converter/DC-motor systems [11], flywheel energy storage systems [12], and nonlinear fractional-order systems [13].

ADRC was first proposed as a nonlinear form, which generally employs nonlinear forms of ESO and SEF. Nonlinear ADRC (NLADRC) has strong antidisturbance and excellent control performance. However, the use of nonlinear functions may make the system produce some complex nonlinear behaviors, such as multiple equilibrium points, limit cycles, bifurcations, and chaos. Meanwhile, stability and performance analyses are very difficult for such nonlinear systems, and too many parameters make the tuning rather difficult, which inhibits the application of ADRC. And many theoretical issues, including its applicability in stabilization and output regulation, remain unanswered. This brings a continuous challenge in the study of the ADRC theory. Therefore, linear ADRC (LADRC) was proposed to overcome these disadvantages by Gao [14]. The previous studies on analyzing stability and performance of

LADRC can be mainly classified into two groups. One is time-domain analysis [15–17], which lays a solid theoretical foundation and provides a strict theoretical support for application. And another is frequency-domain analysis [18, 19], which is significantly important so that the ADRC framework is understood using the almost universal frequency-domain analysis languages shared by practicing control engineers, including both bandwidth and stability margins.

Based on LADRC, some modified ADRC schemes were also developed to improve the control performance. In [20, 21], an ADRC is derived by effectively integrating adaptive control with ESO via the backstepping method. The adaptive law is synthesized to handle parametric uncertainties, and the remaining uncertainties are estimated by the extended state observer and then compensated in a feedforward way. In [22], ADRC for time-delay systems is considered, and a predictive ADRC is established. In [23], a modified ESO with a time-varying gain is proposed, which reduces the "peaking phenomenon" caused by the constant high gain in the traditional ESO. And in [4], a sliding-mode-based component is designed, in order to take into account disturbance estimation errors and uncertainties in the knowledge of the control gain.

Although ADRC theory is widely investigated in previous studies, there are still some problems:

(1) Only sufficient condition for the stability of the ADRC system is proposed.

(2) It failed to explain the reasons for tuning b_0 to increase the robustness of the system and failed to provide theoretical guidance for the tuning of b_0 (b_0 is the nominal high-frequency gain of the plant).

(3) It failed to explain when model information should be applied.

In this paper, these issues will be resolved, and some further deep research results will be presented.

In Section 2, a new structure of ADRC will be shown to illustrate its integral performance. In Section 3, the controller will be transformed into the framework of a two-degree-of-freedom (TDF) internal model control (IMC) to analyze its performance. In Section 4, tuning of some parameters will be discussed to enhance system robustness. In Section 5, simulations are used to verify the effectiveness of the proposed method. Finally, some concluding remarks are drawn in Section 6.

2. ADRC Algorithm

Consider the following typical single-input-single-output (SISO) system:

$$\begin{cases} \dot{x}_1 = x_2, \\ \dot{x}_2 = x_3, \\ \vdots \\ \dot{x}_n = f(1, x2, \ldots, xn, w(t)) + bu, \\ y = x_1, \end{cases} \tag{1}$$

where y is the regulated output, x_i ($i = 1, 2, \ldots, n$) are the system state, u is the input force, b is the high-frequency gain, and $f(x_1, x_2, \ldots, x_n, w(t))$ is the total disturbance including both the model uncertainties and external disturbances.

ADRC generally consists of a tracking differentiator (TD), an extended state observer (ESO), and a state error feedback (SEF). A TD is often used to arrange the transition process to solve the contradiction between system speed and overshoot. The general form of a TD is described as

$$\begin{cases} \dot{v}_1 = v_2, \\ \dot{v}_2 = v_3, \\ \vdots \\ \dot{v}_{n-1} = v_n, \\ \dot{v}_n = \lambda^n \psi\left(v_1 - r, \dfrac{v_2}{\lambda}, \ldots, \dfrac{v_n}{\lambda^{n-1}}\right), \end{cases} \tag{2}$$

where r is the reference input, v_i ($i = 1, 2, \ldots, n$) are the output, and λ is the adjustable speed factor. $\psi(v_1 - r, v_2/\lambda, \ldots, v_n/\lambda^{n-1})$ is a solution that guarantees the fast convergence from v_1 to r.

The ESO, as the core of ADRC, is usually used to estimate system states and total disturbance, and referring to equation (1), an ESO can be usually designed in the following form:

$$\begin{cases} \dot{z}_1 = z_2 - \beta_1 (z_1 - y), \\ \dot{z}_2 = z_3 - \beta_2 (z_1 - y), \\ \vdots \\ \dot{z}_n = z_{n+1} - \beta_n (z_1 - y) + b_0 u, \\ \dot{z}_{n+1} = -\beta_{n+1} (z_1 - y), \end{cases} \tag{3}$$

where z_i ($i = 1, 2, \ldots, n$) are the outputs of the ESO; β_i ($i = 1, 2, \ldots, n$) are the observer gains; and b_0 is the nominal value of b, and $bb_0 > 0$. For the sake of discussion, we assume that $b > 0$.

SEF is used to compensate the total disturbance and eliminate the residual error, and the SEF is designed as

$$\begin{cases} u = \dfrac{u_0 - z_{n+1}}{b_0}, \\ u_0 = \displaystyle\sum_{i=1}^{n} k_i (v_i - z_i), \end{cases} \tag{4}$$

where k_i ($i = 1, 2, \ldots, n$) are the controller gains.

Substituting (4) into (3), we have

$$\begin{cases} \dot{z}_1 = z_2 - \beta_1 (z_1 - y), \\ \dot{z}_2 = z_3 - \beta_2 (z_1 - y), \\ \vdots \\ \dot{z}_n = -\beta_n (z_1 - y) + u_0, \\ \dot{z}_{n+1} = -\beta_{n+1} (z_1 - y). \end{cases} \tag{5}$$

From (5), we can see that z_{n+1} can be expressed as

$$z_{n+1} = \frac{\beta_{n+1}}{\beta_i}\left(z_i - \int z_{i+1}dt\right), \quad 1 \le i \le n-1. \tag{6}$$

When $i = 1$, we have

$$z_{n+1} = \frac{\beta_{n+1}}{\beta_1}\left(z_1 - \int z_2 dt\right). \tag{7}$$

Thus, with a TD and an SEF, the structure of ADRC can be transformed into the form in Figure 1.

Obviously, from Figure 1, we can see that ESO can be considered to be made up of a state observer (SO) and an integrating element. And the SO can be described as

$$\dot{z}_s = A_s z_s + B_s K_s \hat{r} + \beta_s y, \tag{8}$$

where $z_s = [z_1, z_2, \ldots, z_n]^{\mathrm{T}} \in R^n$,

$$A_s = \begin{bmatrix} -\beta_1 & 1 & 0 & \ldots & 0 & 0 \\ -\beta_2 & 0 & 1 & \ldots & 0 & 0 \\ \vdots & \vdots & \vdots & \ddots & \vdots & \vdots \\ -\beta_{n-1} & 0 & 0 & \ldots & 1 & 0 \\ -\beta_n - k_1 & -k_2 & -k_3 & \ldots & -k_{n-1} & -k_n \end{bmatrix} \in R^{n\times n},$$

$$B_s = [0, 0, \ldots, b_0]^{\mathrm{T}} \in R^n,$$

$$K_s = \left[\frac{k_1, k_2, \ldots, k_n}{b_0}\right] \in R^n,$$

$$\beta_s = [\beta_1, \beta_2, \ldots, \beta_n]^{\mathrm{T}} \in R^n,$$

$$\hat{r} = [v_1, v_2, \ldots, v_n]^{\mathrm{T}} \in R^n. \tag{9}$$

Applying Laplace transformation to (8), we can obtain

$$Z_1(s) = \frac{\sum_{j=0}^{n-1}\left(\sum_{i=1}^{n-j-1} k_{i+j+1}\beta_i s^j\right) + \beta_{n-j}s^j}{M(s)} Y(s) + \frac{1}{M(s)}\widehat{R}(s),$$

$$Z_2(s) = \frac{\sum_{j=1}^{n-1}\left(\sum_{i=2}^{n-j-1} k_{i+j}\beta_i s^j\right) + \beta_{n-j+1}s^j - k_1\beta_1}{M(s)} Y(s) + \frac{\beta_1 + s}{M(s)}\widehat{R}(s), \tag{10}$$

where $M(s) = \det(sI - A_s) = s^n + \sum_{i=0}^{n-1}(\beta_{n-i} + \sum_{j=i}^{n-1} k_i\beta_{j-i})s^i$, in which I is the identity matrix. $Y(s)$, $\widehat{R}(s)$, $Z_1(s)$, and $Z_2(s)$ are the Laplace transforms of y, $\hat{r}$, z_1, and z_2, respectively.

According to (7) and (10), we have

$$\begin{aligned} Z_{n+1}(s) &= \frac{\beta_{n+1}}{\beta_1}\left(Z_1(s) - \frac{1}{s}Z_2(s)\right) \\ &= \frac{\beta_{n+1}}{\beta_1}\left(\frac{\beta_1 s^{n-1} + \beta_1\sum_{i=-1}^{n-2} k_{i+2}s^i}{M(s)} Y(s) + \frac{\beta_1}{sM(s)}\widehat{R}(s)\right) \\ &= \frac{\beta_{n+1}}{\beta_1}\left(\frac{\beta_1 s^n + \beta_1\sum_{i=0}^{n-1} k_{i+1}s^i}{sM(s)} Y(s) + \frac{\beta_1}{sM(s)}\widehat{R}(s)\right) \\ &= \frac{\beta_{n+1}}{\beta_1}\left(\frac{M_1(s)}{M(s)} Y(s) + \frac{\beta_1}{M(s)}\widehat{R}(s)\right)\frac{1}{s}, \end{aligned} \tag{11}$$

where $Z_{n+1}(s)$ is the Laplace transform of z_{n+1}. And it can be known from (4) that the feedback of "total disturbance" is completed by the following formula:

$$u' = \frac{z_{n+1}}{b_0}. \tag{12}$$

Although ADRC does not make use of integral directly, it shows that an integral is automatically generated from (12), which provides a good explanation why ADRC has a high steady-state precision. As we know, b_0 can be used as a tuning parameter to improve the control performance of ADRC. However, the tuning of b_0 is generally found by trial and error, and no theory is available to support the method [24].

Remark 1. With (11) and Figure 1, we can see that increasing b_0 can reduce the integral gain; that is, the integral time constant is increased to increase the system robustness. However, if b_0 is too large, the integral action will become so weak that the system will have steady-state deviation. Therefore, we must choose an eclectic b_0.

3. System Performance Analysis

Let the set of transfer functions be

$$P(s) = \frac{l_m s^m + \cdots + l_1 s + l_0}{a_h s^h + \cdots + a_1 s + a_0}, \tag{13}$$

where m and h are positive integers, and all $m \le h$. ADRC does not need the complete models of the controlled plant and the disturbance, but the relative order of $P(s)$; that is, $n = h - m$, $b = l_m/a_h > 0$, and $l_0 \ne 0$.

3.1. System Transformation

Assumption 1. A TD can accurately track the reference input and get its derivatives [18].

Let $z = [z_1, z_2, \ldots, z_n, z_{n+1}]^{\mathrm{T}}$. Then, (3) can be transformed into the following form:

$$\begin{cases} \dot{z} = A_e z + \beta(y - \hat{y}) + Bu, \\ \hat{y} = Cz, \end{cases} \tag{14}$$

where

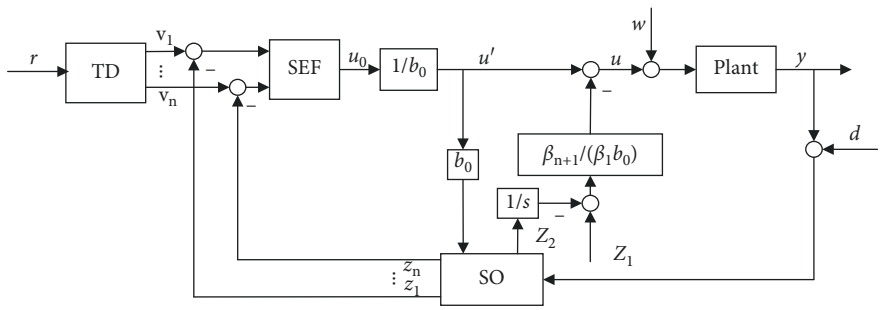

Figure 1: Structure of ADRC. w: total disturbance; d: sensor noise.

$$A_e = \begin{bmatrix} 0 & 1 & 0 & \dots & 0 \\ 0 & 0 & 1 & \dots & 0 \\ \vdots & \vdots & \vdots & \ddots & \vdots \\ 0 & 0 & 0 & \dots & 1 \\ 0 & 0 & 0 & \dots & 0 \end{bmatrix} \in R^{(n+1)(n+1)},$$
$$B = [0, 0, \dots, b_0, 0]^{\mathrm{T}} \in R^{n+1}, \quad (15)$$
$$C = [1, 0, \dots, 0, 0] \in R^{n+1},$$
$$\beta = [\beta_1, \beta_2, \dots, \beta_n, \beta_{n+1}]^{\mathrm{T}} \in R^{n+1}.$$

Substituting (4) into (14), we obtain

$$\begin{cases} \dot{z} = (A_e - \beta C - BK)z + BKv + \beta y, \\ u = K(v - z), \end{cases} \quad (16)$$

where

$$K = \left[\frac{k_1, k_2, \dots, k_n, 1}{b_0}\right] \in R^{n+1},$$
$$v = [v_1, v_2, \dots, v_n, 0]^{\mathrm{T}} \in R^{n+1}. \quad (17)$$

By taking Laplace transform of (16), we have

$$sZ(s) = (A_e - \beta C - BK)Z(s) + BKV(s) + \beta Y(s), \quad (18)$$

$$U(s) = K(V(s) - Z(s)), \quad (19)$$

where $Z(s)$, $U(s)$, and $V(s)$ are the Laplace transforms of z, u, and v, respectively.

Substituting (19) into (18), we have

$$U(s) = \left(1 - K\left(sI - A_e + \beta C + BK\right)^{-1}B\right)KV(s) - K\left(sI - A_e + \beta C + BK\right)^{-1}\beta Y(s). \quad (20)$$

From Assumption 1, we can see that

$$V(s) = \left[1, s, s^2, \dots, s^{n-1}, 0\right]^{\mathrm{T}} R(s) = F(s)R(s), \quad (21)$$

where $R(s)$ is the Laplace transform of r. Thus, (20) can be further transformed into

$$\begin{aligned} U(s) &= \left(1 - K\left(sI - A_e + \beta C + BK\right)^{-1}B\right)KF(s)R(s) \\ &\quad - K\left(sI - A_e + \beta C + BK\right)^{-1}\beta Y(s) \\ &=: \left(1 - KA^{-1}B\right)KF(s)R(s) - KA^{-1}\beta Y(s) \\ &=: C_1(s)R(s) - C2(s)Y(s), \end{aligned} \quad (22)$$

where

$$C_1(s) = \left(1 - KA^{-1}B\right)KF(s),$$
$$C_2(s) = KA^{-1}\beta, \quad (23)$$
$$A = sI - A_e + \beta C + BK.$$

The above result indicates that ADRC can be equivalent to a two-degree-of-freedom internal model control (TDF-IMC), and the TDF-IMC structure is shown in Figure 2.

Remark 2. It can be shown in a similar way to Theorem 1 in [24] that an nth-order ADRC structure shown in Figure 1 can be transformed into a TDF-IMC structure in Figure 2, where P is the plant to be controlled, P_m is the nominal model of P, Q is the tracking IMC controller, Q_{d} is the disturbance rejection IMC controller, and e is the external disturbance.

According to Figure 2, we have

$$U(s) = \frac{Q}{1 - P_m Q_{\mathrm{d}}}R(s) - \frac{Q_{\mathrm{d}}}{1 - P_m Q_{\mathrm{d}}}Y(s). \quad (24)$$

Combined with (22), the following equation can be obtained:

$$Q = \frac{C_1}{1 + P_m C_2},$$
$$Q_{\mathrm{d}} = \frac{C_2}{1 + P_m C_2}. \quad (25)$$

With the configuration in Figure 3, nine transfer functions from $[r, e, d]^{\mathrm{T}}$ to $[u', u, y]^{\mathrm{T}}$ are given by

$$\begin{bmatrix} Q & 0 & 0 \\ \eta Q & -\eta P Q_{\mathrm{d}} & -\eta Q_{\mathrm{d}} \\ \eta PQ & \eta(1 - P_m Q_{\mathrm{d}})P & -\eta P Q_{\mathrm{d}} \end{bmatrix}, \quad (26)$$

where

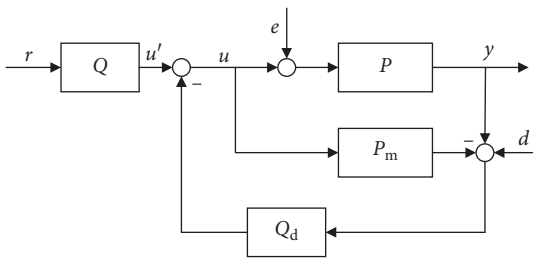

Figure 2: Structure of TDF-IMC.

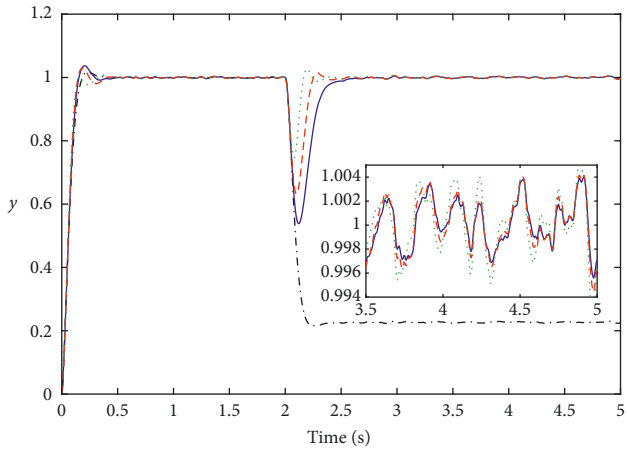

Figure 3: Responses of Example 1 (dash-dot: $k_{n+1} = 0$; solid: $k_{n+1} = 15$; dash: $k_{n+1} = 27.78$; dot: $k_{n+1} = 60$).

$$\eta = \frac{1}{1 + Q_d(P - P_m)}. \tag{27}$$

If the above nine transfer functions are stable, then the closed-loop system is said to be internally stable.

3.2. Stability and Accurate Tracking Performance. For IMC, it is difficult to model accurately. Especially when there is a nonminimum phase part or uncertainty in P, P is very different from P_m. Therefore, the stability of the IMC system is generally proved by the small-gain theorem for simplicity. However, for the IMC transformed by ADRC, we can always let $P_m = P$.

Then, (26) can be transformed into

$$\begin{bmatrix} Q & 0 & 0 \\ Q & -PQ_d & -Q_d \\ PQ & (1 - PQ_d)P & -PQ_d \end{bmatrix}, \tag{28}$$

where Q and Q_d are only related to the parameters β, K, and b_0. In order to simplify parameter tuning, β and K are usually reduced to two tuning parameters as suggested in [14]: ω_c, the controller bandwidth, and ω_o, the extended state observer bandwidth.

Substituting (25) into (28) and considering $C_1 = C_{11}/C_{12}$, $C_2 = C_{21}/C_{22}$, and $P = P_1/P_2$, we have

$$\frac{1}{\delta(s)} \begin{bmatrix} P_2C_{11} & 0 & 0 \\ P_2C_{11} & P_1C_{21} & -P_2C_{21} \\ P_1C_{11} & P_1C_{22} & -P_1C_{21} \end{bmatrix}, \tag{29}$$

where

$$\begin{aligned} \delta(s) &= P_2C_{22} + P_1C_{21}, \\ C_{12} &= C_{22} = \det(A) = Ms, \\ C_{11} &= \left(C_{22} + \det\left(\begin{bmatrix} A & B \\ K & 0 \end{bmatrix}\right)\right)KF(s), \\ C_{21} &= -\det\left(\begin{bmatrix} A & \beta \\ K & 0 \end{bmatrix}\right). \end{aligned} \tag{30}$$

Assumption 2. $M = C_{22}/s$ is Hurwitz.

It can be seen from equation (22) that the calculation of C_{22} is only related to the design parameters of ADRC and has nothing to do with the plant. According to the parameter tuning method in [14], it is easy to guarantee C_{22}/s is Hurwitz.

Theorem 1. *Under Assumption 1 and Assumption 2, for given b_0, $\omega_c > 0$, and $\omega_o > 0$, the closed-loop system is said to be internally stable if and only if $\delta(s)$ is Hurwitz.*

Proof of Sufficiency. If $\delta(s)$ is Hurwitz, then the nine transfer functions of (28) must be stable. For given b_0, $\omega_c > 0$, and $\omega_o > 0$, the closed-loop system is internally stable. □

Proof of Necessity. For given b_0, $\omega_c > 0$, and $\omega_o > 0$, there are no zero roots in C_{11} and C_{21}.

And if Assumption 2 holds, neither C_1 nor C_2 have unstable zeros and unstable poles that can cancel each other out; that is, C_1 and C_2 are both coprime polynomials.

If the closed-loop system is internally stable, then the nine transfer functions of (28) must be stable, and the reason why $\delta(s)$ is Hurwitz is as follows.

Assume that $\delta(s)$ is not Hurwitz and one of the transfer functions of (28), such as

$$Q = \frac{P_2C_{11}}{P_2C_{22} + P_1C_{21}}, \tag{31}$$

whose numerator and denominator contain an identical factor $(s + s^*)$, and $\mathrm{Re}(s^*) \le 0$. If $(s + s^*)$ exists in P_2, then it must exist in C_{21} (i.e., $s^* \neq 0$) as $P(s)$ is a coprime polynomial. And since $M = C_{22}/s$ is Hurwitz, $(s + s^*)$ does not exist in P_1C_{22}; then,

$$(1 - PQ_d)P = \frac{P_1C_{22}}{P_2C_{22} + P_1C_{21}} \tag{32}$$

is unstable. Similarly, if $(s + s^*)$ exists in C_{11}, (29) will also be unstable. In fact, as long as $\delta(s)$ is not Hurwitz, no matter which one of the nine transfer functions is unstable, it will cause at least one transfer function of (28) to be unstable, Q.E.D. □

Remark 3. Theorem 1 is not able to determine internal stability when Assumption 3 does not hold, but sC_1, sC_2, and $P(s)$ are all stable. However, this situation is rare, and it is easy to assure that C_{22}/s is Hurwitz when $\omega_c > 0$ and $\omega_o > 0$. If we exclude such a situation, the condition that $\delta(s)$ is Hurwitz is not only sufficient but also necessary for internal stability. In this sense, we call it an almost necessary and sufficient condition for internal stability.

In the engineering application, the system should have better tracking performance and dynamic performance besides the requirements of the internal stability. From (28), it can be seen that the main channel transfer function can be described as

$$QP = \frac{P_1 C_{11}}{P_2 C_{22} + P_1 C_{21}}. \tag{33}$$

Since $C_{22} = Ms$, it is clear that the coefficient of s^0 of C_{22} is zero, as long as C_{11} and C_{21} contain constants and no zeros of $P(s)$ are located at origin in the complex plane, and the static gain of the main channel function is only determined by the constant terms C_{11} and C_{21}, but not related to C_{22} and $P(s)$:

$$C_{11} = \frac{\left(\sum_{j=0}^{n+1} \beta_{n+1-j} s^j\right)\left(\sum_{i=1}^{n} k_i s^{i-1}\right)}{b_0}, \tag{34}$$

$$C_{21} = \frac{\sum_{j=0}^{n} s^j \sum_{i=1}^{j+1} \beta_{n+i-j} k_i}{b_0}. \tag{35}$$

Theorem 2. *Under Assumption 2, for given b_0, $\omega_c > 0$, $\omega_o > 0$, and all $P \in \wp$, the closed-loop system is said to have accurate tracking performance if and only if $\delta(s)$ is Hurwitz.*

Proof of Sufficiency. If $\delta(s)$ is Hurwitz, then no zeros of $P(s)$ are located at origin in the complex plane. And according to (34) and (35), we have

$$\lim_{s \longrightarrow 0} \frac{P_1 C_{11}}{P_2 C_{22} + P_1 C_{21}} = 1. \tag{36}$$

According to Theorem 1, the closed-loop system is internally stable, and then the closed-loop system has accurate tracking performance. □

Proof of Necessity. If the closed-loop system has accurate tracking performance, then (36) must be established and the closed-loop system is internally stable. According to Theorem 1, $\delta(s)$ is Hurwitz, Q.E.D.

In practical applications, not only should the stability of the system be known but also its stability margin and attenuation ability to the disturbance are required. According to Theorem 1, the stability of the ADRC system is determined by $\delta(s)$, while its attenuation ability to disturbance and sensor noise is determined by pQ_{d} (as can be seen from Figure 2 and (28)). □

Corollary 1. *Under Assumption 2, for given b_0, $\omega_c > 0$, and $\omega_o > 0$, the closed-loop system is said to be internally stable if pQ_d is stable and C_{21} is Hurwitz.*

Proof. From (29), we can see that

$$pQ_{\mathrm{d}} = \frac{P_1 C_{21}}{\delta(s)} = \frac{P_1 C_{21}}{P_2 C_{22} + P_1 C_{21}}. \tag{37}$$

If Q_{d} is stable and C_{21} is Hurwitz, then $\delta(s)$ is Hurwitz because there are no unstable zeros and unstable poles to cancel each other out, and then the closed-loop system is internally stable based on Theorem 1. □

Corollary 2. *Under Assumption 2, when $n \le 4$, for given b_0, $\omega_c > 0$, and $\omega_o > 0$, the closed-loop system is said to be internally stable if and only if pQ_d is stable.*

Before proof, the following lemma is given.

Lemma 1 [25]. *Polynomial $\varphi(s)$ is Hurwitz if $\mu_i \le 0.4655$ or $\mu_i + \mu_{i+1} \le 0.89$ $(p \ge 5)$, where*

$$\varphi(s) = \alpha_0 s^p + \alpha_1 s^{p-1} + \cdots + \alpha_p,$$
$$\mu_i = \frac{\alpha_i \alpha_{i+3}}{\alpha_{i+1} \alpha_{i+2}}. \tag{38}$$

Let $C_{21} = \varphi(s)$ and $\omega_c = \theta \omega_o$, $\theta > 0$.

Proof.

(1) When $n = 1$ or 2, α_i are all positive, so C_{21} is Hurwitz.

(2) When $n = 3$,

$$\begin{aligned}
\mu_0 &= \frac{\alpha_0 \alpha_3}{\alpha_1 \alpha_2} \\
&= \frac{\left(4\theta^3\omega_{\mathrm{o}}^6 + 3\theta^2\omega_{\mathrm{o}}^6\right)\left(6\theta^3\omega_{\mathrm{o}}^5 + 12\theta^2\omega_{\mathrm{o}}^5 + 3\theta\omega_{\mathrm{o}}^5\right)}{\left(4\theta^3\omega_{\mathrm{o}}^4 + 18\theta^2\omega_{\mathrm{o}}^4 + 12\theta\omega_{\mathrm{o}}^4 + \omega_{\mathrm{o}}^4\right)\theta^3\omega_{\mathrm{o}}^7} \\
&= \frac{4\theta^3 + 18\theta^2 + 12\theta + 1}{24\theta^3 + 66\theta^2 + 48\theta + 9} \\
&< \frac{4\theta^3 + 18\theta^2 + 12\theta + 1}{3.66\left(4\theta^3 + 18\theta^2 + 12\theta + 1\right)} \\
&< \frac{1}{3.66} < 0.4655.
\end{aligned} \tag{39}$$

(3) When $n = 4$, we have

$$\begin{aligned}
\mu_0 &< \frac{1}{3.5} < 0.4655, \\
\mu_1 &< \frac{1}{2.52} < 0.4655.
\end{aligned} \tag{40}$$

Table 1: Tuning methods for b_0.

	$P(s)$	b_0
1	$\forall a_i > 0\,(i = 1, 2, \ldots, h)$ but $\exists l_i < 0\,(i = 1, 2, \ldots, m)$	Increasing b_0
2	$\exists a_i \le 0\,(i = 1, 2, \ldots, h)$ but $\forall l_i \ge 0\,(i = 1, 2, \ldots, m)$	Decreasing b_0
3	$\exists a_i < 0\,(i = 1, 2, \ldots, h)$ and $\exists l_i < 0\,(i = 1, 2, \ldots, m)$	More model information should be used

Therefore, based on Lemma 1, when $n \le 4$, C_{21} is Hurwitz. Then, the necessary and sufficient condition of Corollary 2 is easy to be proved. □

Remark 4. When $n = 5$,

$$\mu_0 < \frac{1}{3.4} < 0.4655,$$
$$\mu_1 < \frac{1}{2.23} = 0.448, \tag{41}$$
$$\mu_2 < \frac{1}{1.98} = 0.505.$$

$\mu_1 + \mu_2$ may be greater than 0.89 for $\exists\theta > 0$. In fact, it is not hard to find by calculation that as n increases, the minimum value of the upper bound of μ_i increases for $\forall\theta > 0$. But C_{21} may still be Hurwitz because Lemma 1 is only a sufficient condition. Therefore, it is necessary to determine whether C_{21} is Hurwitz, when $n \ge 5$.

Remark 5. According to (28) and (37), the greater the bandwidth of pQ_d, the stronger the antidisturbance capability of the ADRC system and the greater the influence of the sensor noise.

Remark 6. When C_{21} is Hurwitz, according to Corollary 1 and Corollary 2, the stability margin of pQ_d can reflect the stability margin of the ADRC system to some extent. And it can be seen from (25) that pQ_d can be considered a closed-loop transfer function whose open-loop transfer function is P_mC_2. In this way, we can use frequency-domain analysis to analyze P_mC_2 so as to determine the stability of the whole ADRC system.

4. Parameter Tuning

ADRC parameter tuning has always been an important topic because of a bunch of parameters. For practical purposes, the parameters of ADRC are simplified to ω_c and ω_o [14]. However, sometimes b_0 is also adjusted as the third parameter to improve system performance because of unknown information on b and robustness requirement. But before this article, there were no specific theoretical principle and theoretical guidance for the tuning of b_0. In fact, a solution to this problem was proposed in Remark 6, i.e., to solve this problem with frequency-domain analysis of P_mC_2.

However, in practice, model information is sometimes difficult to know accurately. Therefore, a more concise method is needed to guide the tuning of b_0. According to the

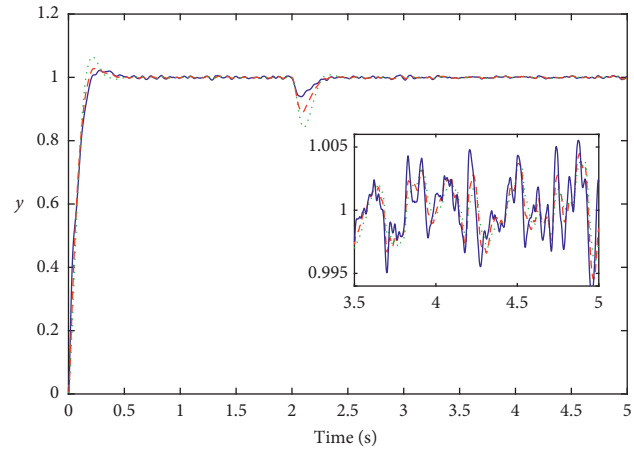

Figure 4: Responses of $\eta = 5$ (solid: $b_0 = 3$; dash: $b_0 = 5$; dot: $b_0 = 7$).

Routh criterion, a necessary condition for $\delta(s)$ to be Hurwitz is that the coefficients of $\delta(s)$ have the same symbol and are not zero. When the symbol of the coefficients in (13) is known, in order to guarantee the establishment of this necessary condition, the tuning methods are used, which are listed in Table 1.

The methods about how to incorporate more plant information in ADRC are described in the study of Tan and Fu [24, 26].

Moreover, it can be seen from (7) and Figure 1 that the integral function of ADRC is only related to z_{n+1}, so in order to make the ADRC parameter more explicit, referring to Figure 1, $\beta_{n+1}/\beta_1 b_0$ is replaced with k_{n+1} as a separated adjustable parameter. In this way, z_{n+1} can be considered a separate integrating element, and k_{n+1} can be viewed as an approximate integral gain to adjust.

So, the number of parameters of the ADRC can be expanded to four: ω_c, the controller bandwidth; ω_o, the observer bandwidth; b_0; and k_{n+1}, the approximate integral gain, where ω_c and ω_o are the same as in [14]. Then, (34) and (35) can be transformed into

$$C_{11} = \frac{c_{2n}s^{2n} + \cdots + c_1 s}{b_0} + k_1\beta_1 k_{n+1},$$
$$C_{21} = \frac{q_n s^n + \cdots + q_1 s}{b_0} + \cdots k_1\beta_1 k_{n+1}, \tag{42}$$

where $c_1 = q_1 \ne 0$ as $\omega_c > 0$ and $\omega_o > 0$.

Obviously, (36) is still valid; that is, if $\delta(s)$ is Hurwitz, the closed-loop system still has accurate tracking performance.

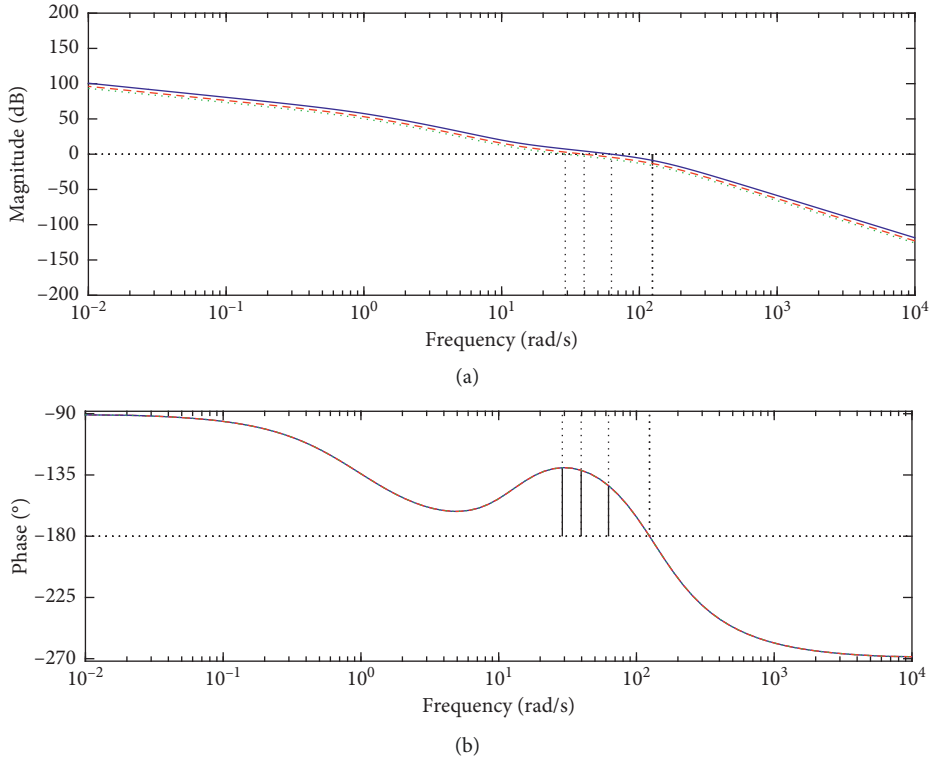

Figure 5: Bode diagram of $P_m C_2$ when $\eta = 5$ (solid: $b_0 = 3$; dash: $b_0 = 5$; dot: $b_0 = 7$).

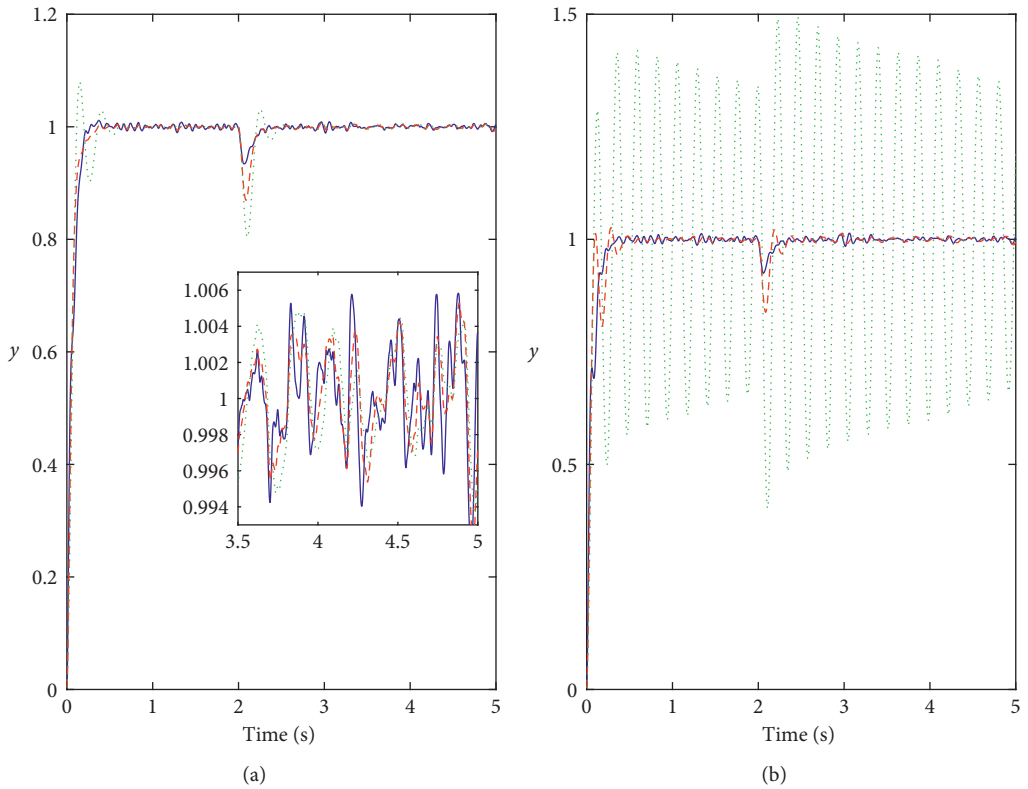

Figure 6: Responses of (a) $\eta = -5$ and (b) $\eta = -15$ (solid: $b_0 = 3$; dash: $b_0 = 5$; dot: $b_0 = 7$).

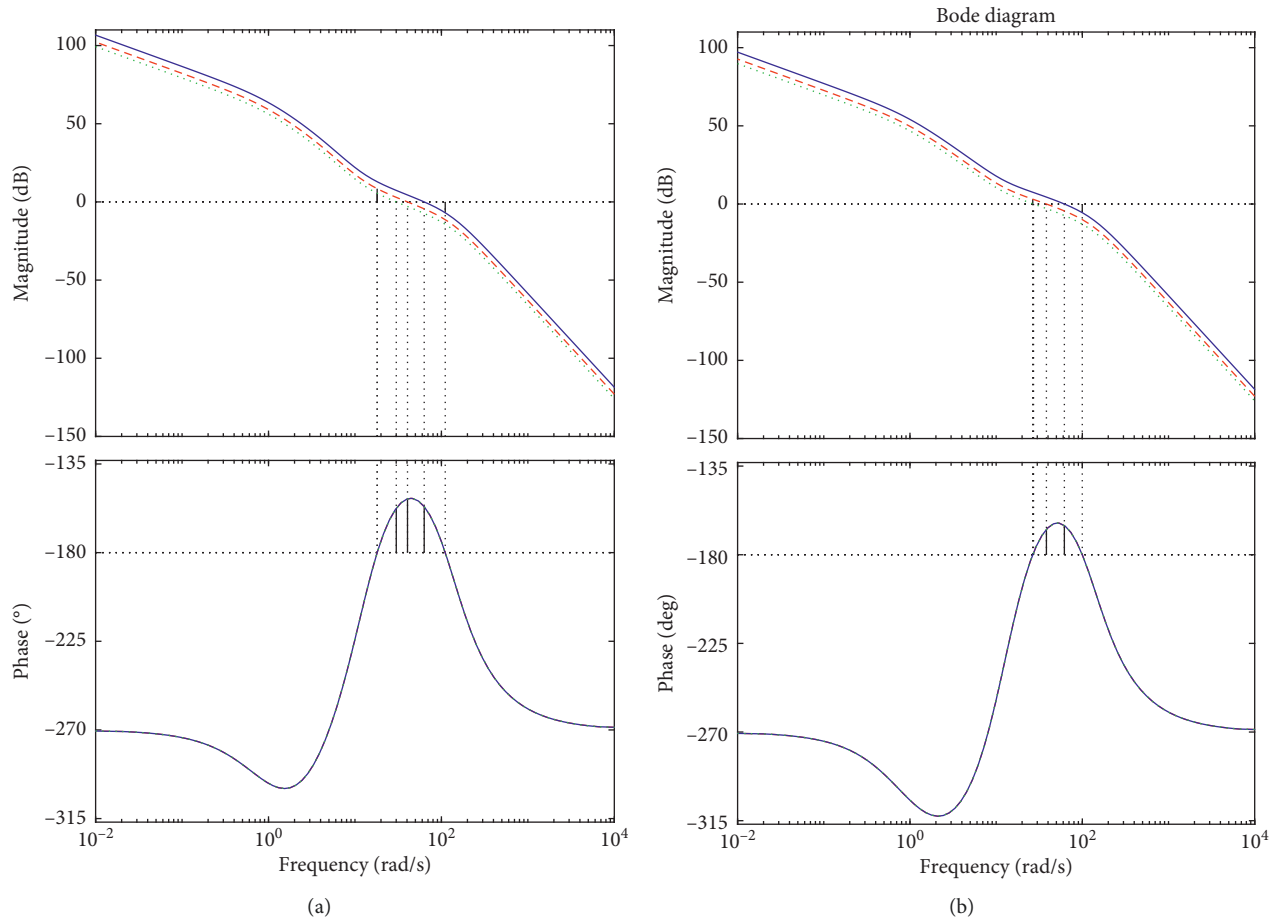

Figure 7: Bode diagram of $P_m C_2$ when (a) $\eta = -5$ and (b) $\eta = -15$ (solid: $b_0 = 3$; dash: $b_0 = 5$; dot: $b_0 = 7$).

5. Simulation

Example 1. The practical model of the simulation in this section is used in [14, 24, 27, 28]. The estimated mathematical model of the motion control system is

$$\ddot{y} = -1.41\dot{y} + 23.2T_d + 23.2u, \tag{43}$$

where y is the output position, u is the control voltage sent to the power amplifier, and T_d is the torque disturbance. The corresponding second-order ADRC is designed, and the parameters are tuned as

$$\begin{aligned} \omega_c &= 30, \\ \omega_o &= 50, \\ b_0 &= 40, \\ \frac{\beta_{n+1}}{\beta_1 b_0} &= 27.78. \end{aligned} \tag{44}$$

For a better view of the comparison among different values of k_{n+1}, the four values $k_{n+1} = 0, k_{n+1} = 15, k_{n+1} = 35.92$, and $k_{n+1} = 60$ are selected. The responses of the ADRC system are shown in Figure 3 for a step reference, the step disturbance with an amplitude of −10 is injected at $t = 2$ seconds, and a 0.1% white noise in the sensor is added (this noise is added to all examples). The sampling time is 1 kHz. It is shown that as k_{n+1} increases, the system's antidisturbance capability increases, and the impact of noise increases (but the increase is small). In fact, the adjustment range of k_{n+1} is very large, and the system becomes unstable when $k_{n+1} > 300$. Therefore, in terms of increasing the system's antidisturbance capability, larger k_{n+1} should be chosen. In addition, when $k_{n+1} = 0$, the system can accurately track the step input before $t = 2$, but after the step disturbance is injected, the accurate tracking performance of the system is lost, which shows that the integral effect of ADRC is only related to z_{n+1}.

Example 2. Consider a second-order plant

$$G_1 = \frac{5}{(s+1)(s+\eta)}, \tag{45}$$

where η is unknown. In this simulation, the tuning parameters are set as

$$\omega_c = 30,$$
$$\omega_o = 50, \quad (46)$$
$$k_{n+1} = \frac{\beta_{n+1}}{\beta_1 b_0}.$$

The responses for a step reference at $t = 0$ and a step input disturbance with an amplitude of -20 at $t = 2$ are shown.

For $\eta = 5$, it can be seen from Figure 4 that as b_0 increases, the system's antidisturbance capability decreases, but the effect of sensor noise also decreases. Based on Figure 5, it is clear that as b_0 increases, the cutoff frequency of $P_m C_2$ is reduced; that is, the bandwidth of pQ_d is reduced, which is why both the system's antidisturbance capability and the influence of sensor noise are reduced. Further simulation results show that increasing b_0 can also improve the robustness of the system because the amplitude margin and phase margin of $P_m C_2$ increase. In addition, for the minimum phase system, increasing b_0 will not change the phase-frequency characteristic of $P_m C_2$. But only the overall downshift of the amplitude-frequency characteristic curve is caused. Therefore, within a certain range, increasing b_0 will necessarily increase the amplitude margin and phase margin.

For $\eta = -5$ and $\eta = -15$, comparing (a) and (b) in Figures 6 or 7, we can see that the robustness and antidisturbance capability of the system decrease as b_0 increases, which is consistent with the description of Case 2 in Table 1. In fact, it is known by the Bode stability criterion that when $\eta < -15$, the system of $b_0 = 7$ becomes unstable; when $\eta < -24$, the system of $b_0 = 5$ becomes unstable; and when $\eta < -34$, the system of $b_0 = 3$ becomes unstable.

6. Conclusion

In this paper, the linear ADRC method was investigated. The integral effect of the ADRC was analyzed under the premise that ADRC was transformed into a new form. Then, ADRC was changed into an IMC framework, and an almost necessary and sufficient condition for stability and tracking performance of ADRC systems have been proposed on this basis. In addition, some useful corollaries have been proposed so that the traditional open-loop frequency-domain analysis method can be applied to ADRC system stability analysis. Furthermore, it also provides a theoretical principle and theoretical guidance for tuning of b_0. To improve the performance of ADRC, k_{n+1} (the approximate integral gain) was treated as a separated adjustable parameter according to the new structure. Finally, simulations were used to verify the effectiveness of b_0 and k_{n+1} tuning methods. Future research efforts include the extension of the results to nonlinear systems and the practical applications of the proposed approach.

Data Availability

The data used to support the findings of this study are available from the corresponding author upon request.

Conflicts of Interest

The authors declare that they have no conflicts of interest.

Acknowledgments

This work was supported by the National Natural Science Foundation of China (61501429).

References

[1] J. Han, "Active disturbance rejection controller and its applications," *Control Decision*, vol. 13, no. 1, pp. 19–23, 1998, in Chinese.

[2] J. Han, "From PID to active disturbance rejection control," *IEEE Transactions on Industrial Electronics*, vol. 56, no. 3, pp. 900–906, 2009.

[3] M. Ran, Q. Wang, and C. Dong, "Active disturbance rejection control for uncertain nonaffine-in-control nonlinear systems," *IEEE Transactions on Automatic Control*, vol. 62, no. 11, pp. 5830–5836, 2017.

[4] F. Alonge, M. Cirrincione, F. DIppolito, M. Pucci, and A. Sferlazza, "Robust active disturbance rejection control of induction motor systems based on additional sliding-mode component," *IEEE Transactions on Industrial Electronics*, vol. 64, no. 7, pp. 5608–5621, 2017.

[5] Q. Zhong, J. Wu, Y. Zhang, and J. Yang, "Non-linear auto-disturbance rejection control of parallel active power filters," *IET Control Theory & Applications*, vol. 3, no. 7, pp. 907–916, 2009.

[6] L. Dong, Y. Zhang, and Z. Gao, "A robust decentralized load frequency controller for interconnected power systems," *ISA Transactions*, vol. 51, no. 3, pp. 410–419, 2012.

[7] T. Ali, "Boundary control of a circular curved beam using active disturbance rejection control," *International Journal of Control*, vol. 92, no. 5, pp. 1–18, 2017.

[8] K. Erenturk, "Fractional-order $PI^{\lambda}D^{\mu}$ and active disturbance rejection control of nonlinear two-mass drive system," *IEEE Transactions on Industrial Electronics*, vol. 60, no. 9, pp. 3806–3813, 2013.

[9] H. Sira-Ramirez, J. Linares-Flores, C. Garcia-Rodriguez, and M. A. Contreras-Ordaz, "On the control of the permanent magnet synchronous motor: an active disturbance rejection control approach," *IEEE Transactions on Control Systems Technology*, vol. 22, no. 5, pp. 2056–2063, 2014.

[10] C. H. A. Criens, F. P. T. Willems, T. A. C. van Keulen, and M. Steinbuch, "Disturbance rejection in diesel engines for low emissions and high fuel efficiency," *IEEE Transactions on Control Systems Technology*, vol. 23, no. 2, pp. 662–669, 2015.

[11] J. Linares-Flores, J. L. Barahona-Avalos, H. Sira-Ramirez, and M. A. Contreras-Ordaz, "Robust passivity-based control of a buck-boost-converter/DC-motor system: an active disturbance rejection approach," *IEEE Transactions on Industry Applications*, vol. 48, no. 6, pp. 2362–2371, 2012.

[12] X. Chang, Y. Li, W. Zhang, N. Wang, and W. Xue, "Active disturbance rejection control for a flywheel energy storage system," *IEEE Transactions on Industrial Electronics*, vol. 62, no. 2, pp. 991–1001, 2015.

[13] Z. Gao, "Active disturbance rejection control for nonlinear fractional-order systems," *International Journal of Robust and Nonlinear Control*, vol. 26, no. 4, pp. 876–892, 2016.

[14] Z. Gao, "Scaling and bandwidth-parameterization based controller tuning," in *Proceedings of the 2003 American*

Control Conference, pp. 4989–4996, Denver, CO, USA, June 2003.

[15] Q. Zheng, L. Gao, and Z. Gao, "On validation of extended state observer through analysis and experimentation," *Journal of Dynamic Systems, Measurement, and Control*, vol. 134, no. 2, article 024505, 2012.

[16] S.-S. Chen, Y.-Z. He, and T.-S. Dong, "Structure influence on the robust stability of linear active disturbance rejection control system," in *Proceedings of the 2016 35th Chinese Control Conference (CCC)*, pp. 67–72, Chengdu, China, July 2016.

[17] F. Wang, E.-H. Liu, R.-J. Wang, W.-M. Zhang, and Y.-L. Yang, "An approach to improve active disturbance rejection control," *International Journal of Control*, pp. 1–11, 2018.

[18] W. Xue and Y. Huang, "On frequency-domain analysis of ADRC for uncertain systems," in *Proceedings of the 2013 American Control Conference*, pp. 6637–6642, Wanshington, DC, USA, June 2013.

[19] G. Tian and Z. Gao, "Frequency response analysis of active disturbance rejection based control system," in *Proceedings of the 2007 IEEE 22nd International Symposium on Intelligent Control*, pp. 1595–1599, Singapore, October 2007.

[20] J. Yao and D. Wenxiang, "Active disturbance rejection adaptive control of uncertain nonlinear systems: theory and application," *Nonlinear Dynamics*, vol. 89, no. 3, pp. 1611–1624, 2017.

[21] J. Yao and W. Deng, "Active disturbance rejection adaptive control of hydraulic servo systems," *IEEE Transactions on Industrial Electronics*, vol. 64, no. 10, pp. 8023–8032, 2017.

[22] Q. Zheng and Z. Gao, "Predictive active disturbance rejection control for processes with time delay," *ISA Transactions*, vol. 53, no. 4, pp. 873–881, 2014.

[23] Z. L. Zhao and B. Z. Guo, "On active disturbance rejection control for nonlinear systems using time-varying gain," *European Journal of Control*, vol. 23, pp. 62–70, 2015.

[24] T. Wen and C. Fu, "Linear active disturbance-rejection control: analysis and tuning via IMC," *IEEE Transactions on Industrial Electronics*, vol. 63, no. 4, pp. 2350–2359, 2015.

[25] K. Jiang, "Xie and Nie stability criterion," *Information and Control*, vol. 1, no. 7, pp. 34–38, 1983, in Chinese.

[26] S. Zhao, L. Sun, D. Li, and Z. Gao, "Tracking and disturbance rejection in non-minimum phase systems," in *Proceedings of the 33rd Chinese Control Conference*, pp. 3834–3839, Nanjing, China, July 2014.

[27] D. Yoo, *Optimal tracking condition for linear extended state observer on uncertain system*, Ph.D thesis, University of Illinois, Chicago, IL, USA, 2005.

[28] D. Yoo, S. S.-T. Yau, and Z. Gao, "Optimal fast tracking observer bandwidth of the linear extended state observer," *International Journal of Control*, vol. 80, no. 1, pp. 102–111, 2007.